NATURAL CONVECTION ON VERTICAL FLAT PLATES: A NUMERICAL AND EXPERIMENTAL STUDY.

Rodrigo Carrijo Lino[*]
rodrigocarrijo@bol.com.br

Douglas Machado Ramos[*]
duglasmramos@hotmail.com

José Luiz Alves da Fontoura Rodrigues[*]
fontoura@unb.br

* Universidade de Brasília – Departamento de Engenharia Mecânica – 70910-900 - DF

Abstract. *The aim of this work is a numerical and experimental study of the natural convection heat transfer on a vertical flat plate, subjected to a constant heat flux. The experimental study was performed on an experimental setup designed in order to assuming, with a good approximation, those adopted natural convection hypotheses on a heated vertical flat plate. The experimental setup is constituted by one glass reservoir with 560 mm long, 470 mm height and 130mm width. The heated vertical flat plate, measuring 315 mm height and by 35 mm width was made in aluminium, having in its interior a heat source made of thermo-foil heaters, with dimensions of 25,4mm x 152,4 mm each, a nominal electrical resistance of 20.8 , and 12A of maximum electrical current. The numerical simulation of the flow, made by the CFX-5.5.1 code from the AEA Technology, solves the flow respecting the geometry, the initial and boundary conditions utilized in the laboratory. The turbulent models used are the **k-w** of Wilcox (1998) and the SST of Menter (1993). The obtained results are represented by means of correlations that show the variations of local Nusselt number in function of local Rayleigh number. The numerical and experimental results obtained, show a good proximity when compared to the empirical-dimensional and analytical previsions for laminar and transition natural convection.*

Keywords. Natural laminar and transition convection, vertical flat plate, constant heat flux, experimental analysis, numerical analysis.

1. Introduction

Natural convection on verticals walls is a physical phenomenon strongly associated to the human activity. Both, generation and use, of the thermal energy and the thermal comfort, are areas where this kind of phenomenon is widely present.

The most common situation, where natural convection appears, is when body forces act in a fluid with density gradients. As result of the action of the gravitational force, in a stratified fluid, there appears a buoyancy force that causes a natural convection flow. Usually the density gradient is due to the temperature gradients.

The origin of natural convection is an unstable situation, resulting from the orientation of the temperature gradient. However, a flow will only occur, when the buoyancy forces defeats the dissipative effect of the viscous forces.

Several techniques and process of solution had been developed for the qualitative and quantitative analysis of convection, amongst which one may to make reference to experimental techniques, pure theoretical analysis and numerical simulation. Empirical approaches based on scaling analysis and finished by experimental information, and most recently, numerical simulations techniques, arisen to the computational advances, have been used in the study of natural convection. The works of Bejan (1984), Kays and Crawford (1980) and Burmeister (1983) are examples of the most usual solutions, of laminar, transition and turbulent natural convection, based in theoretical, numerical and scaling analysis. The works of Qureshi and Gebhart (1978), Vliet and Liu (1969) and Goldstein and Eckert (1960) are classical works in the experimental investigation on laminar, transition and turbulent natural convection on a uniformly heated vertical plate.

The aim of this work is the study of the natural convection on a vertical flat plate, subjected to a constant heat flux, in contact with a stagnant water reservoir. Three kinds of analysis were used in this work: experimental approach, scaling analysis and numerical simulation. This study begins, with an analysis of the scales of the terms appearing on the governing equations, which are used to drive the experiments and the numerical methods, to verify the experimental and numerical results as well to establish the relation between the Nusselt and Rayleigh numbers. Seven different flows, obtained for different intensities of the heat flux on the vertical plate, were analyzed.

The use of the numerical simulation, in this work, has as objective to evaluate the capacity of a industrial computer code, in the prediction of the laminar and the beginning of transition flow in natural convection.

2. Governing Equations and Scaling Analysis

We suppose a water steady state flow on a vertical flat and impermeable plate, subjected to no-slip wall conditions and to a constant heat flux through the wall. The fluid in the reservoir is initially considered stationary and isothermal. The Boussinesq hypothesis is used to model the buoyancy effects.

The typical scales, of the hydrodynamic and thermal boundary layer, should be defined. A typical scale for length, in a perpendicular direction to the wall, is the thermal boundary layer thickness, δ_T, and a scale for length, along the tangent direction to the wall, is the length of the flat plate H, where H $\gg$ δ_T. The representative scales for the velocity and temperature gradients are considered to obey the following relations:

$$\frac{\partial v}{\partial x} >> \frac{\partial v}{\partial y}, \frac{\partial u}{\partial x}, \frac{\partial u}{\partial y}, \tag{1}$$

and

$$\frac{\partial T}{\partial x} >> \frac{\partial T}{\partial y}, \tag{2}$$

where x and y are the independent position variables, respectively, in the perpendicular direction to the wall and in the tangent direction to the wall, u and v the velocity components along these directions and T is the temperature.

From equation (1) it is possible to affirm that the only important component of the shear stress is:

$$\boldsymbol{t}_{xy} = \boldsymbol{t}_{yx} = \boldsymbol{m}\left(\frac{\partial v}{\partial x}\right), \tag{3}$$

where τ_{xy} and τ_{yx} are the shear stresses and μ the molecular viscosity. Due to equation (2), the rates of diffusion heat flux, normal to the wall, has a higher magnitude than the longitudinal ones.

An evaluation of the orders of magnitude of the component terms of the general equations, representative of the mass conservation, momentum conservation and energy conservation, considering the typical scales of the hydrodynamic and thermal layers, condensed by the relationships (1), (2) and (3), under the restrictions of the approach of Boussinesq for natural convection, gives the following equations in Cartesian coordinates for the natural convection on a vertical flat plate:

$$\frac{\partial}{\partial x}\left(\boldsymbol{r}_0 u\right) + \frac{\partial}{\partial y}\left(\boldsymbol{r}_0 v\right) = 0, \tag{4}$$

$$\frac{\partial p}{\partial x} = 0, \tag{5}$$

$$\frac{\partial}{\partial x}\left(\boldsymbol{r}_0 uv\right) + \frac{\partial}{\partial y}\left(\boldsymbol{r}_0 vv\right) = \frac{\partial}{\partial x}\left(\boldsymbol{m}\frac{\partial v}{\partial x}\right) + \boldsymbol{r}_0 g\boldsymbol{b}\left(T - T_\infty\right), \tag{6}$$

$$u\frac{\partial T}{\partial x} + v\frac{\partial T}{\partial y} = \boldsymbol{a}\frac{\partial^2 T}{\partial x^2}. \tag{7}$$

The conservation principles of mass, momentum and energy are expressed by equations (4), (5), (6) and (7). Equations (5) and (6) are the momentum equations in the longitudinal and the transverse directions respectively. The pressure is represented by p and T_∞ is the external temperature, out of the thermal boundary layer. The fluid properties such as the density $\boldsymbol{r}_0$, the molecular viscosity $\boldsymbol{m}$ and the thermal diffusivity $\boldsymbol{a}$ are assumed constant. The gravitational acceleration is represented by g. The sole property that is allowed to change with temperature is β, the thermal expansion coefficient. It represents the effect of the local variation of the density of the fluid, which will be used strictly on the buoyancy term of equation (6).

Besides that, it is important to establish an order of magnitude for the difference of temperature:

$$\Delta T \approx \Theta = T_W - T_\infty. \tag{8}$$

The subscript $_W$ represents the values that are assumed at the wall. The heat flux q is modeled by the Fourrier Law, in terms of the length and temperature scales:

$$q \approx k\frac{\Delta T}{\boldsymbol{d}_T}. \tag{9}$$

In the above equation, k represents the thermal conductivity.

The scale analysis for natural convection starts on the study of the momentum equation, equation (6). This equation shows the existence of three different types of forces: inertia force, friction force and buoyancy force, this last one being the most important force of the flow. The order of magnitude of these three forces scales as,

$$inertia \sim \frac{v^2}{H}, \qquad friction \sim \frac{vu}{d_T^2}, \qquad buoyancy \sim gb\Delta T,$$

where H represents the vertical length of the plate and υ the kinematics viscosity of the fluid. To characterize, the relative dimensions of these forces, we make a relation of the three magnitude orders with the scale of the buoyancy force: $g\beta\Delta T$. The result obtained from this procedure is shown, in a convenient way, as

$$inertia \sim \left(\frac{H}{d_T}\right)^4 Ra^{-1} Pr^{-1}, \qquad friction \sim \left(\frac{H}{d_T}\right)^4 Ra^{-1}, \qquad buoyancy \sim 1,$$

where Pr and Ra represent the numbers of Prandtl and the total number of Rayleigh, defined respectively by the equations

$$Pr = \frac{u}{a} \qquad \text{and} \qquad Ra = \frac{gb\Delta TH^3}{au}.$$

The order of magnitude of the inertia forces, friction forces and buoyancy forces, expressed as a function of the scale of the buoyancy forces, shows that the Prandtl number defines the competition between inertia forces and friction forces. For fluids with high values of Prandtl number, the buoyancy forces should balance the friction forces, since inertia forces are negligible. Fluids with low values of the Prandtl number will originate flows where the buoyancy forces should balance mainly inertia forces.

As the fluid to be analyzed is the water, which, under usual pressure and temperature conditions, has a Prandtl number around 6, only the results for Prandtl numbers greater than 1 will be shown. For this condition, the scales for the velocity components u and v, as well as the relation between the thickness of the hydrodynamic boundary layer δ and the thermal boundary layer δ_T, (δ /δ_T), and the Nusselt number are shown in the Table 1. These are presented as functions of the thermal diffusivity α, the flat plate length H, the total Rayleigh number Ra and the Prandtl number Pr.

Table 1. Order of magnitude of the most important variables.

Natural Convection on a flat plate subjected to a constant heat flux.				
Prandtl number >>1 ; buoyancy forces $\approx$ friction forces				
U	v	δ_T	δ /δ_T	Nu
$u \approx \dfrac{a}{H} Ra^{\frac{1}{5}}$	$v \approx \dfrac{a}{H} Ra^{\frac{1}{5}}$	$d_T \approx HRa^{\frac{1}{5}}$	$\dfrac{d}{d_T} \approx Pr^{\frac{1}{2}}$	$Nu \approx Ra^{\frac{1}{5}}$

The relations defined on Table 1 were used to guide the construction of the experimental setup and they were important, as well, to the calibration of the sensors used to acquire significant data. These results will be essential to establish a relation between the local Nusselt number, defined as hy/k, and the local Rayleigh number.

3. Experimental Analysis

3.1 Experimental Installation

The experimental setup is composed by four main components: a water reservoir made of glass, a vertical aluminum flat plate, a heating system and a data acquisition system, as shown on the figure 1.

The dimensions of the reservoir are 470 x 560 x 130mm (height, width and depth). Twelve cooper-constantan thermocouples are used to measure the temperature along the plate and two are used to evaluate the temperature of the reservoir, far from the thermal boundary layer.

The thermocouples are distributed on the center line of the flat plate and were numbered from the leading edge to the top of the flat plate, as shown in table 2.
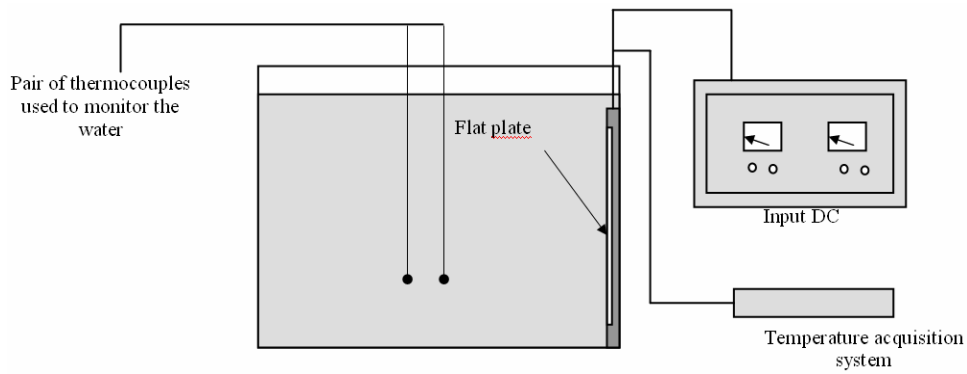
Figure 1. Experimental setup.

Table 2. Thermocouple distribution along the flat plate.

Thermocouple	Distance from the beginning of the board (mm)
1	2
2	5
3	10
4	15
5	20
6	25
7	30
8	50
9	100
10	200
11	250
12	290
13	Thermocouples used to monitor the water temperature
14	

This implies that the energy that is introduced into the plate by these thermo-foils, will be dissipated only by the wet face. The thermo foil heaters are supplied by a constant voltage. The figure 2 shows with details of the assembly of the plate. A DaqBooK data acquisition system is used for the acquisition, treatment and storage of the thermocouple signals. The description of the installation is the following: a TCA 120-20 Tectrol electric current stabilizer of 2400 W power and voltage band from 0 to 120 V, current band from 0 to 20 A; Omega Engineering thermocouples copper-constantan of 0.1 mm diameter; Embrapol polyester resin with catalyser concentration of 1%; Iotech DaqBok 112 DBK19 acquisition board, with a DaqView 7.8.0 Iotech acquisition software; Minco HK5335R20.8L12A 876 thermo foil heater, with 25,4 mm x 152,4 mm, with electric resistance of 20.8 Ω and maximum current of 12A. Figure 2 shows the details of the assembly of the flat plate.
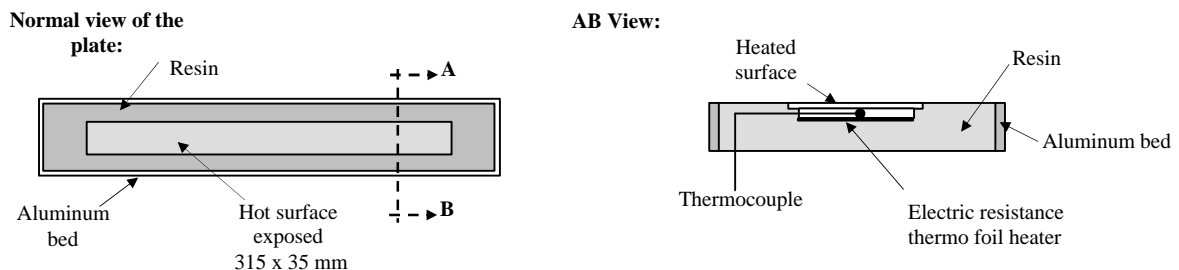

Figure 2. Flat plate details.

3.2 Experimental Methodology

The used experimental methodology is based on the measurement of the $T_W(y)$ temperature that establishes on the heated vertical flat plate. This temperature is caused by the heat generated by Joule effect in the electric resistances. It is transmitted to the plate and, consequently, to the fluid in the reservoir. At steady state, the heat dissipated by the

electric resistances is absorbed by the aluminum flat plate and is transmitted integrally to the fluid on the reservoir, by convection. At these conditions, the equation of the convective heat flux per area unit, allows to calculate the local convective heat transfer coefficient h as

$$h_y = \frac{q}{(T_W(y) - T_\infty)} \quad , \tag{10}$$

where the specified heat flux q is known and the temperatures of the wall $T_W(y)$ and of the reservoir T_∞ are measured by the thermocouples. The variations of the flow along the flat plate are presented, under non-dimensional form, in terms of a local Nusselt number and local Rayleigh number correlation. It is intended to determine a correlation expression as follows:

$$Nu_y = cRa_y{}^n , \tag{11}$$

where the local Nusselt number and the local Rayleigh number are, respectively, calculated by:

$$Nu_y = \frac{hy}{k} , \tag{12}$$

$$Ra_y = \frac{gby^4 q}{auk} . \tag{13}$$

The experiments were carried on for different heat flux intensities in the wall and the data acquisition started when the flow reached the steady state. Therefore, at this condition, the thermocouple temperature signals were constant for each heat flux condition. The statistical treatment of the data was based on twenty realizations for each experiment, with five 5 seconds each and 10 Hz of acquisition system. It could then be determined an average value for the temperature for each thermocouple, associated to a standard deviation. The statistical treatment given to the acquired data, determined for each experiment, is the average value of the temperature and its standard deviation for each thermocouple. These values were calculated, respectively, by the following relations:

$$\overline{T_i} = \frac{\sum\limits_{j=1}^{N} T_j}{N} , \tag{14}$$

$$T_i' = \sqrt{\frac{\sum\limits_{j=1}^{N} (\overline{T_i} - T_j)^2}{N-1}} . \tag{15}$$

In the above equations N means the number of acquisition data, and the subscript i specifies the thermocouple. The table 3 shows the conditions for the seven experiments.

Table 3. Heat fluxes used during the experimental acquisition.

Experiment	Heat Flux (W/m²)	Dissipated power (W)	Battery Voltage (V)
1	1000	11,01	21,4
2	1500	16,23	26,2
3	2000	22,05	30,3
4	2500	27,56	33,9
5	3000	33,08	37,1
6	5000	55,13	47,8
7	10000	110,25	67,7

The physical properties of the water were taken at 300 K in accordance with Incropera and De Witt (1990): $k = 0,613$ W/mK, $\mu = 855 \times 10^{-6}$ Ns/m², $\rho = 997$ Kg/m³, $g = 9,81$ m/s², $\beta = 2,761 \times 10^{-4}$ K^{-1}, Pr = 5,83.

4. Numerical analysis

The qualities of numerical results that can be obtained nowadays, especially with industrial tools, justify the use of numerical simulations, with turbulence models, in the design of the experimental facilities.

The used software is CFX 5.5.1 of AEA Technology, with two turbulence models to simulate the free convection on flat plate. Due to the flow complexity, especially in the proximities of the hot surface, turbulence models that do not use the wall laws were selected. The employed turbulence models were the Wilcox κ-ω (1998) and the SST of Menter (1993), which is an improvement of the Wilcox model (1998). The superiority of the results obtained for these models, especially with the SST of Menter (1993), compared to the results obtained with the κ-ε model of Jones and Launder (1972) complemented by wall laws, which is not efficient near the walls, are verified by the works of Leschziner et. al. (1999) and Bardina et. al. (1997).

The aim of this work is not to study turbulence models. Thus, the SST and κ-ω models are shown in way to evidence their specific characteristics only, what allows to omit the turbulent Reynolds averaged equations of continuity and momentum. These last are the same for all first order closure problems based on the turbulence's Bousinesq (1877) hypothesis. It should be stressed out that, despite we consider numerical simulations with turbulence models, the simulations of the laminar and the transition regions are not affected, since the eddy diffusion coefficients are proportional to the turbulence intensity.

The turbulent modeling, of the convection problem, is made with the introduction of a buoyancy term in the average momentum equation. The density variations are modeled by the Boussinesq hypothesis to free convection and are associated to a state equation for density. The correlation of temperature and velocity fluctuation is calculated as a linear function of the average temperature. The modeling of turbulent heat flux is based on the work of Kader (1981).

In this work, two-dimensional and three-dimensional simulations have been done. The boundary conditions for the two-dimensional one are: for the heated flat plate a no-slip condition with constant heat flux is used; on the base of the domain and on the face opposite to the flat plate, the no-slip condition is used and a fixed temperature is imposed. This was also proposed for the upper boundary for the domain, but now with a free slip condition. It should be noted that for these three last boundaries, the heat transfer coefficient was also specified. The specification of the heat transfer coefficient was done with the simplified equations for air given by empirical relations for free convection proposed by McAdams (1954). In this work the mesh used for the numerical two-dimensional simulation had 68.667 nodes, 249.774 elements and 104.814 faces, which is show in the figure 3. In this picture is available a zoom of a near wall region.

For the three-dimensional simulation, the boundary conditions of the left and right vertical walls of reservoir are: a no-slip condition and a specified temperature. For the other boundaries, the same conditions for the two-dimensional simulations were used. The three-dimensional simulation was performed in order to reproduce the experimental setup described on section 3. For this simulation the mesh had 197163 nodes, 1106614 elements, 1106614 tetrahedrons and 30916 faces. For this mesh a picture is not shown.
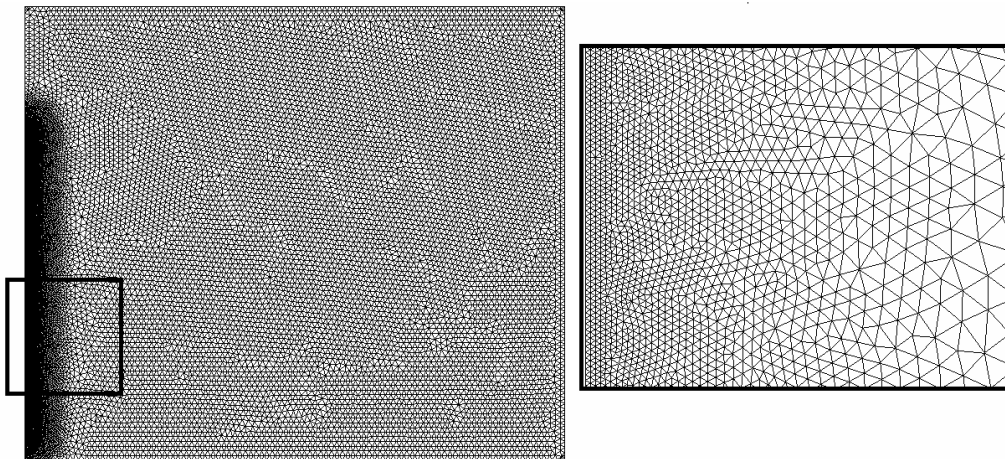

Figure 3. Mesh with zoom in the wall region.

4.1 The k-w Model

The κ-ω model of Wilcox (1998) is a first order closure problem, based on the Boussinesq (1877) hypothesis for representation of the Reynolds tensor, where the turbulent length scales are

$$u_t = \frac{k}{w},$$ (16)

where υ_t is the kinematics eddy viscosity, κ the turbulence kinetic energy and ω the specific dissipation of turbulence kinetic energy. The introduction of two variables in the system composed by averaged equations, that describes the

flow, imposes the adoption of the transport equations for κ and ω. These variables characterize the Wilcox (1998) turbulence model:

$$\frac{\partial(rk)}{\partial t} + \nabla \circ [r\mathbf{U}k] = P_k - b'rkw + \nabla \circ \left[\left(m + \frac{m_t}{s_k}\right)\nabla k\right],$$

(17)

$$\frac{\partial(rw)}{\partial t} + \nabla \circ [r\mathbf{U}w] = x\frac{w}{k}P_k - brw^2 + \nabla \circ \left[\left(m + \frac{m_t}{s_w}\right)\nabla w\right].$$

(18)

In equations (17) and (18), $\mathbf{U}$ is the velocity vector, μ_t is the turbulent viscosity, P_k is turbulence production rate, defined by

$$P_k = m_t 2\underline{\underline{S}} : \nabla \mathbf{U},$$

(19)

where $\underline{\underline{S}}$ is strain rate tensor and β', β, ξ, σ_k and σ_ω are the constant of the model and are considered, in the CFX, to assume the following values:

$$b' = 0{,}09, \quad b = \frac{3}{40}, \quad x = \frac{5}{9}, \quad s_k = 2 \text{ e } s_w = 2.$$

4.2 SST Model

The model SST is a improvement of the κ-ω model of Wilcox (1998), based on the representation of the eddy viscosity through the relationship

$$u_t = \frac{a_1 k}{\max(a_1 w, SF_2)},$$

(20)

where F2 is a function defined just in the boundary layer and S is the value of the shear rate. In this model, the function F2 is defined as

$$F_2 = \tanh\left[\max\left(\frac{2\sqrt{k}}{b'wy}, \frac{500m}{y^2 w}\right)\right]$$

(21)

5. Results

The results were presented in curves that show the local Nusselt number, equation (12), as a function of the local Rayleigh number, equation (13), both calculated in terms of the distance from the leading edge of the vertical flat plate. The experimental results are showed in comparison with the numerical results, corresponding to the simulate values obtained with the turbulence models κ-ω of Wilcox (1998) and SST of Menter (1993), with the 2D grid illustrated by figure 3. These results were also compared to analytical results, calculated by the expression proposed by Sparrow (1955), which was obtained by an integral analysis for natural convection in vertical flat plate, submitted to constant heat flux. This expression is the following

$$Nu_y = \frac{2}{360^{\frac{1}{5}}}\left(\frac{\Pr}{\frac{4}{5} + \Pr}\right)^{\frac{1}{5}} Ra_y^{\frac{1}{5}}.$$

(22)

The figures 4, 5, 6 and 7 correspond, respectively, to the experiments with constant heat flux specified in the wall of 1000 W/m², 1500 W/m², 2000 W/m², 2500 W/m², 3000 W/m², 5000 W/m² and 10000 W/m². The beginning of transition region, in all the experiments, occurred for values of local Rayleigh number approximately 10^{12}, according the results of Qureshi and Gebhart (1978) and Vliet and Liu (1969). In the laminar region, an excellent agreement between experimental, numerical and analytical values is observed, for all heat fluxes imposed.

For all the seven experiments, in the proximity of the transition region, $Ra_y \approx 10^{12}$, a growing up divergence is observed, between the experimental and the analytical results, and it increases for higher values of local Rayleigh

number. For $Ra_y \approx 10^{12}$ in the figure 7(a) takes place the maximum difference observed, between the experimental and the analytical values of Nusselt number, arriving up to 23%.

A very good agreement between the experimental and the numerical results was verified for the results shown on figures 4(a) to 6(b). This confirms the capacity of the Menter's SST model (Menter, 1993) to simulate the behavior of the fluid observed experimentally. For the highest value of heat flux, shown in figure 7(a), the numerical values obtained by the κ-ω model of Wilcox (1998) provide a good agreement for the laminar region of the flow. However, as Ra_y increases, one can observe errors up to 30%. For this case, the experimental and numerical results, obtained with the SST model of Menter (1993), shown to diverge up to 14% for values of Ra_y larger than 3×10^{11}.
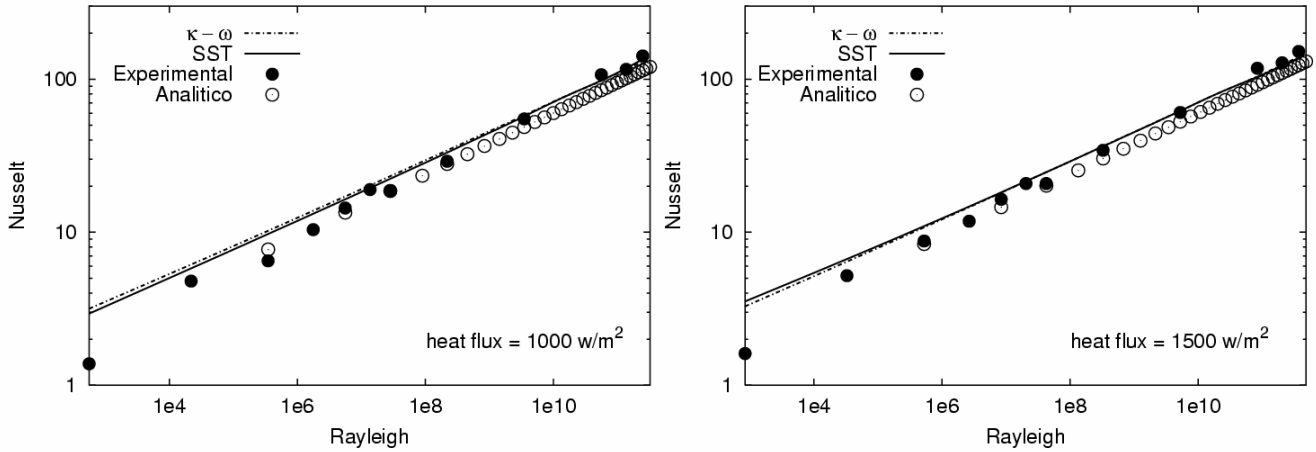
Figure 4. (a) Experiment 1, constant heat flux of 1000 W/m^2. (b) Experiment 2, constant heat flux of 1500 W/m^2.
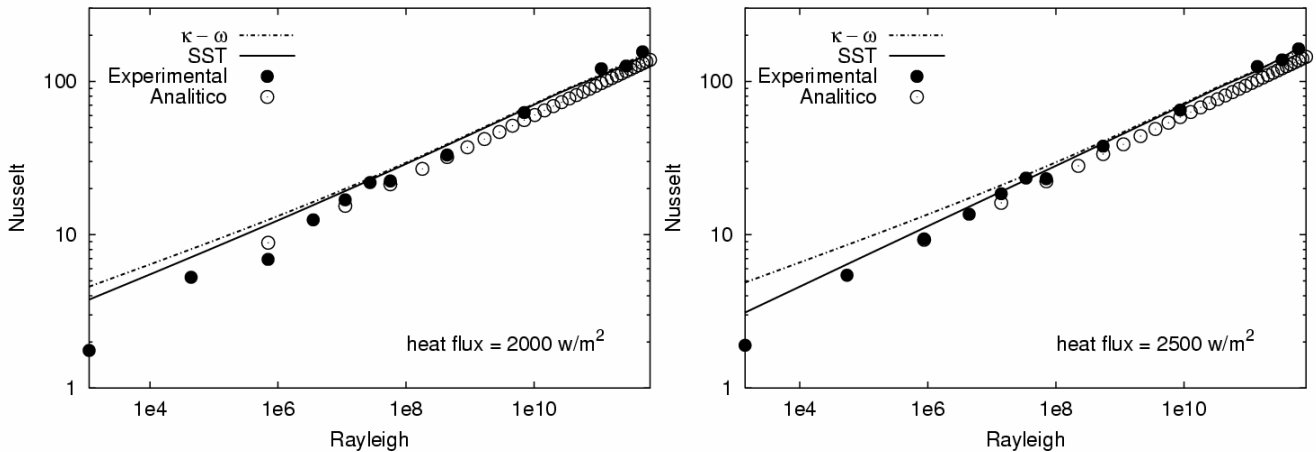

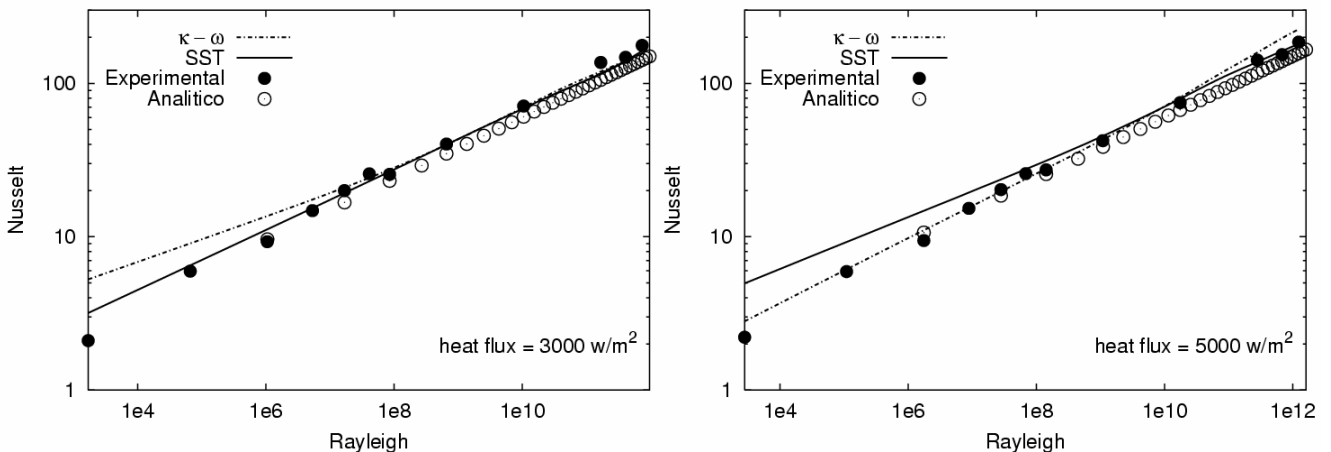Figure5. (a) Experiment 3, constant heat flux of 2000 W/m^2. (b) Experiment 4, constant heat flux of 2500 W/m^2.

Figure 6. (a) Experiment 5, constant heat flux of 3000 W/m^2. (b) Experiment 6, constant heat flux of 5000 W/m^2.

It could be observed, in general, the good capacity of the model SST of Menter (1993) to describe the beginning of transition and all laminar region.

The figure 7(b) shown all the experimental results obtained. It could be observed that the variation of local Nusselt number does not depend on the wall heat flux in the laminar region. In the begin of the transition region, $Ra_y \approx 10^{12}$, the dependence of the Nusselt number with the heat flux is not sensible in the figure 7(b), however the experimental data indicate this tendency.

For the experiments 1 to 6, the coefficient 'c' presented in equation (11), was calculated for the numerical results and for the experimental results. The values obtained for these coefficients were in good agreement. The value found with the experimental data is 0.72 while the numerical results lead to 0.71. The results obtained by Qureshi and Gebhart (1978) and Vliet and Liu (1969) are respectively 0.587 and 0.64.
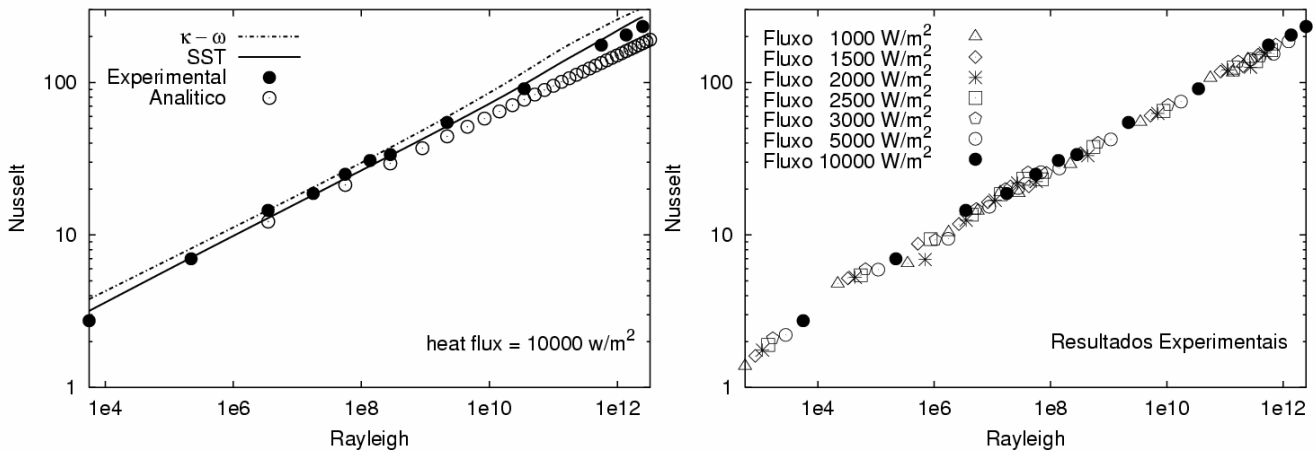

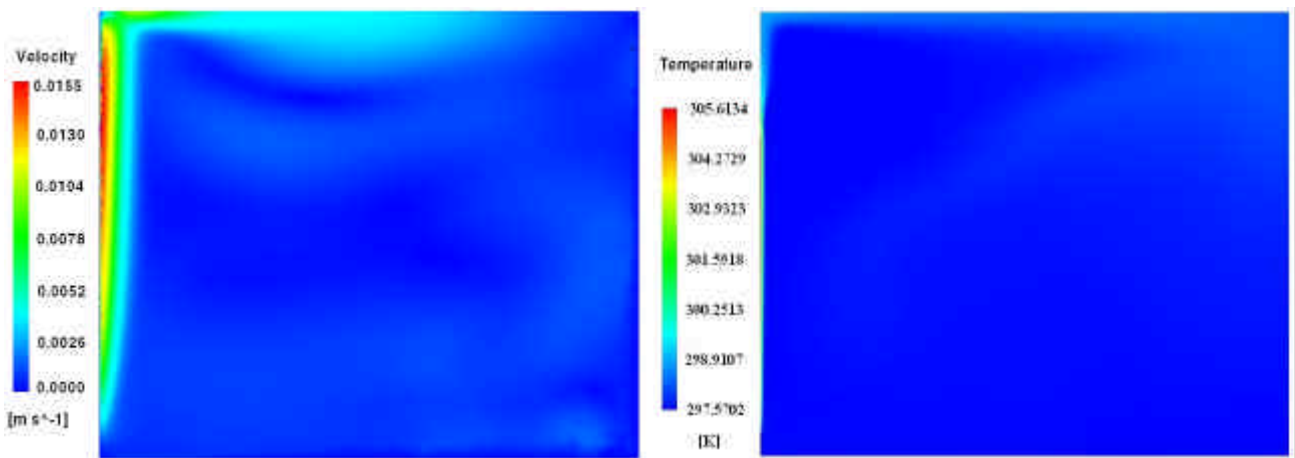Figure 7. (a) Experiment 7, constant heat flux of 10000 W/m^2. (b) Experimental results.

Figure 8. (a) Velocity field for stagnant reservoir. (b) Temperature field for stagnant reservoir.

The velocity and the temperature fields presented in figures 8(a) and 8(b), calculated with the 3D grid, shows that the reservoir is actually stagnant and isothermal, as it was expected. Those results confirm that the reservoir was correctly designed for the study of natural convection on a flat plate. If the velocity intensities were significant, this would become a problem of cavity with recirculation flow.

6. Conclusions

It was verified a good agreement among the experimental, the numerical and the analytical results for both laminar and the beginning of transition regimes, in the first six experiments and in the majority of the results obtained in the seventh experiment. Thus it allows us to conclude that the methodology and the experimental equipment employed in this work are consistent and the proposed objective was attained.

The analytical results proposed by the classic relation of Sparrow (1955) are practically identical to the numerical and experimental results in the laminar region of the flow ($Ra_y < 10^{12}$).

The experimental data has shown the invariability of local Nusselt number with the heat flux in the laminar regime of the flow and the tendency of dependence of the Nusselt number with the heat flux in the beginning of transition region.

7. Acknowledgement

8. References

Bardina, J. E., Huang, P.G., Coakley, T.J., 1997, "Turbulence modeling validation", AIAA, n° 97, pp 2121.

Bejan, A., 1984, "Convection heat transfer", A Wiley-Interscience Publication, John Wiley and Sons, Inc., New York.

Boussinesq, J., 1877, "Théorie de l'écoulement tourbillant", Mem. Présentés ppour diver savants Acad. Sci. Int. France, vol23, pp 46-50, Paris.

Burmeister, L.C., 1983, "Convective heat transfer", A Wiley-Interscience Publication, John Wiley and Sons, Inc., New York.

Goldenstein, R.J., Eckert, E.R.G., 1960, "The steady and transient free convection boundary layer on a uniformly heated vertical plate", International Journal of Heat and Mass Transfer, vol. 1(2-3), pp. 208-210.

Incropera, F.P., De Witt, D.P., 1990, "Fundamentos da transferência de calor e de massa", LTC – Livros Técnicos e Científicos S. A..

Jones, W. and Launder, B., 1972, "The prediction of laminarization with a two equations model of turbulence", International Journal of Heat and Mass Transfer, vol. 15, pp. 301-304.

Kader, B.A., 1981, "Temperature and concentration profiles in fully turbulent boundary layers", International Journal of Heat and Mass Transfer, vol. 24(9), pp. 1541-1544.

Kays, W.M., Crawford, M.E., 1980, "Convective heat and mass transfer", second edition, McGraw-Hill Book Company, New York.

Lsechziner, M.A., Batten, P., Loyau, H, 1999, "Modeling shock-affected near-wall flows with anisotropy-resolving turbulence closures", Proceedings of the 4th International Symposium on Engineering Turbulence Modeling and Measurements, Ajaccio, Córsega.

McAdams, W.C., 1954, "Heat transmission", third edition, McGraw Hill, New York.

Menter, F.R., 1993, "Zonal two equation κ-ω turbulence models for aerodynamic flows", AIAA, n° 93, pp 2906.

Qureshi, Z.H., Gebhart, B., 1978, "Transition and transport in buoyancy driven flow in water adjacent to a vertical uniform flux surface", International Journal of Heat and Mass Transfer, vol. 21(12), pp. 1467-1479.

Sparrow, E.M., 1955, "Laminar free convection on a vertical plate with prescribed nonunform wall heat flux or prescribed nonuniform wall temperature", NACA TN 3508.

Vliet, G.C., Liu, C.K., 1969, "An experimental study of turbulent natural convection boundary layers", Journal of Heat Transfer, vol. 92, pp 517-531.

Wilcox, D.C., 1998, "Turbulence modeling for CFD", second edition, DCW Industries, Inc., Palm Drive, La Canada, California.